

Improved Monte Carlo tree search (MCTS) formulation with multiple root nodes for discrete sizing optimization of truss structures

Fu-Yao Ko, Katsuyuki Suzuki and Kazuo Yonekura

Abstract

This paper proposes a new method for discrete optimum design of truss structures utilizing Monte Carlo tree search (MCTS) with update process, the best reward, accelerating technique, and terminal condition. An improved MCTS formulation with multiple root nodes is developed in this study. Update process means that once a final solution is found, it is used as the initial solution for next search tree. The best reward is used in the backpropagation step. Accelerating technique is introduced by decreasing the width of search tree and reducing maximum number of iterations. The agent is trained to minimize the total structural weight under various constraints until the terminal condition is satisfied. Then, optimal solution is the minimum value of all solutions found by search trees. These numerical examples show that the agent can find optimal solution with low computational cost, stably produces an optimal design, and is suitable for practical engineering problems.

KEYWORDS

Truss optimization; discrete design variables; reinforcement learning; Monte Carlo tree search; update process

1. Introduction

Structural optimization is one of the most important and challenging problems in modern structural design. The primary goal of structural optimization is to find minimum weight of the structures satisfying the performance and construction criteria by the specifications and design codes (Haftka and Gürdal [1992](#); Christensen and Klarbring [2009](#)). The large number of design variables, the highly irregular search space, and a great number of design constraints are main preventive factors in performing optimum design in a reasonable time. The optimization algorithms can be divided into two general categories: traditional mathematical optimization algorithms (Templeman and Yates [1983](#); Duan [1986](#); John, Ramakrishnan, and Sharma [1987](#); Yonekura and Kanno [2010](#)) and metaheuristic algorithms (Rajeev and Krishnamoorthy [1992](#); Altay, Cetindemir, and Aydogdu [2024](#)).

Reinforcement learning (RL) is an interdisciplinary area of machine learning (ML) that focuses on the relationship between an agent and its environment. An RL method aims to train an action taker called agent to take actions to maximize the cumulative

rewards. The training of an agent can be regarded as a trial-and-error process, and the agent gradually learns how to map different states to optimal actions (Sutton and Barto 2018). Monte Carlo tree search (MCTS) is a heuristic search algorithm used to solve sequential decision problems. MCTS builds a search tree according to the simulation results through random sampling (Browne et al. 2012). MCTS method has many applications like game playing, planning, security, chemical synthesis, scheduling, vehicle routing, and so on (Świechowski et al. 2023).

In recent years, RL algorithm has been extensively used in structural optimization problems. Hayashi and Ohsaki (2020) proposed a ML-based method using Q-learning and graph embedding (GE) for binary truss topology optimization. Hayashi and Ohsaki (2021) presented a novel method combining RL and metaheuristic algorithms for optimal design of planar steel frames. Zhu et al. (2021) proposed the concept of machine-specified ground structures for topology optimization of trusses determined from RL and GE. Kupwiat, Hayashi, and Ohsaki (2022) developed a combined method of deep deterministic policy gradient and graph convolutional network for bracing direction optimization of grid shells. Ororbia and Warn (2022) presented a framework that modeled optimal design synthesis as a Markov decision process (MDP) and solved with Q-learning. Zhu et al. (2022) proposed a framework using RL and GE for critical element identification and demolition planning of frame structures. Ororbia and Warn (2023) extended MDP framework using deep Q-network when the structural design domain is relatively large. Kupwiat, Hayashi, and Ohsaki (2024) developed a novel method for solving multi-objective optimization problems using multi-agent RL and graph representation.

MCTS is used to solve truss optimization problems. Luo et al. (2022a) introduced a two-stage MCTS-based RL method to generate the optimal truss layout considering continuous member size, shape, and topology. Luo et al. (2022b) developed MCTS-based RL algorithm to deal with continuous action spaces for truss layout design problems by using kernel regression.

The RL task is modeled as an MDP, where the state transition and reward are solely dependent on the state and the action taken at the current step. The key elements in an MDP framework include agent, environment, state, action, state transition, and reward. The state represents the description of the current truss structure. The only action for this problem is to determine cross-sectional areas of the members. The environment transitions to a new state after taking an action based on the current state. Reward functions describe how the agent ought to behave. For this problem, only the reward for terminal state is considered.

In this paper, an improved MCTS formulation with multiple root nodes is developed for optimal design of truss structures. Update process means that once a final solution

is determined, this solution is utilized as the initial solution for the next search tree. The agent is trained to minimize the weight of the truss under multiple constraints until the terminal condition is satisfied. Then, optimal solution is the minimum value of all solutions found by search trees during the algorithm.

The remainder of this article is constructed as follows. Section 2 briefly presents mathematical model of truss sizing optimization problems with discrete variables. In Section 3, a framework including MCTS with update process, the best reward, accelerating technique, and terminal condition is introduced. In Section 4, convergence history, accuracy, and stability of the present method in finding optimal truss structures are demonstrated. Finally, the conclusions of this study are discussed in Section 5.

2. Discrete optimum design of truss structures: Formulation

A structural optimization problem with discrete design variables can be formulated as a nonlinear programming problem with multiple nonlinear constraints associated with structural behavior. In discrete sizing optimization problems, the main task is to select the cross-sectional areas of the truss members. All of them are selected from a permissible list of standard sections. The optimization problem aims to minimize the weight of the truss while stress and displacement constraints are fulfilled. The optimization design problem for discrete variables can be expressed as follows:

$$\text{Find } \begin{aligned} &\mathbf{X} = (X_1, X_2, \dots, X_i, \dots, X_g), \\ &X_i \in \mathbf{D}, \mathbf{D} = \{d_1, d_2, \dots, d_h, \dots, d_b\} \end{aligned} \quad (1a)$$

$$\text{Minimize } W(\mathbf{X}) = \rho \sum_{i=1}^g \left(X_i \sum_{j=1}^{m_i} L_{i,j} \right) \quad (1b)$$

where \mathbf{X} is the vector containing the design variables, which are selected from a list of available discrete values; $W(\mathbf{X})$ is the weight of the truss; ρ is the material density; g is the number of member groups (design variables); X_i is the cross-sectional area of the members belonging to group i ; m_i is the number of members in the group i ; $L_{i,j}$ is the length of the member j in the group i ; \mathbf{D} is the list including all available discrete values arranged in ascending sequences; h is the index of permissive discrete variables; and b is the number of available sections. The constraints can be formulated as follows:

$$\mathbf{K}(\mathbf{A})\mathbf{u} = \mathbf{F} \quad (2a)$$

$$\varepsilon_{i,j} = \mathbf{B}_{i,j} \mathbf{u}_{i,j} \quad (2b)$$

$$\text{Subject to } \sigma_{i,j} = \frac{E}{L_{i,j}} \varepsilon_{i,j} \quad (2c)$$

$$\sigma_{\min} \leq \sigma_{i,j} \leq \sigma_{\max}, i = 1, 2, \dots, g, j = 1, 2, \dots, m_i \quad (2d)$$

$$\delta_{\min} \leq \delta_k \leq \delta_{\max}, k = 1, 2, \dots, c \quad (2e)$$

where $\mathbf{K}(\mathbf{A})$ is the global stiffness matrix of the structure; \mathbf{u} is a vector containing the displacements of the non-suppressed nodes of the truss; \mathbf{F} is a vector containing the applied forces at these nodes; $\varepsilon_{i,j}$ is the elongation of the member; $\mathbf{B}_{i,j}$ is defined as $\mathbf{B}_{i,j} = (-\mathbf{e}'_{i,j} \quad \mathbf{e}'_{i,j})$; $\mathbf{e}_{i,j}$ is a unit vector along the member so that it points from local node 1 to local node 2; $\mathbf{u}_{i,j} = (\mathbf{u}_{i,j}^1 \quad \mathbf{u}_{i,j}^2)'$ is a vector including the displacements of the end points of the member; E is the modulus of elasticity; and c is the number of structural joints. Figure 1 shows the notation for a truss optimization problem.

From Equations (2d) and (2e), the stress $\sigma_{i,j}$ in each member of the truss is compared with the allowable stresses σ_{\min} and σ_{\max} . The displacement δ_k of node k of the truss is compared with the allowable displacements δ_{\min} and δ_{\max} .

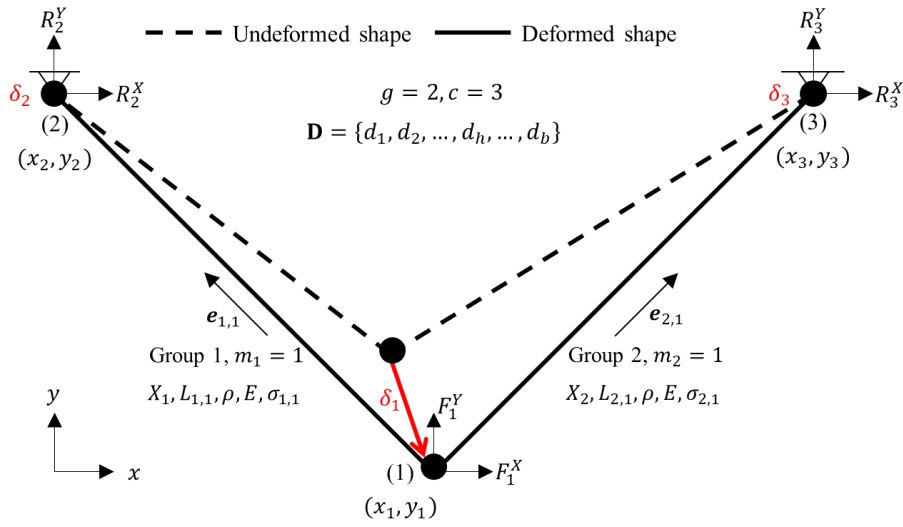


Figure 1. 2-bar planar truss for the notation of truss optimization problem.

3. MCTS with update process, the best reward, accelerating technique, and terminal condition for discrete optimum design of truss structures

3.1. MDP for structural optimization

Figure 2 illustrates the MDP used in this research. At each time step t , the agent observes the state s_t as numerical data of nodes and members representing the truss structure, as shown in Figure 2(a). Then, it takes the action a_t to determine the member area. Figure 2(b) shows that the cross-sectional area X_1 is changed from d_b to d_h . When the agent transitions to a new state, it receives a reward r_{t+1} computed from the truss optimization problem, as shown in Figure 2(c). MDP model can be represented by a tree structure with $(g + 1)$ layers, including state (Section 3.1.1), action (Section 3.1.2), and state transition (purple line), as shown in Figure 3.

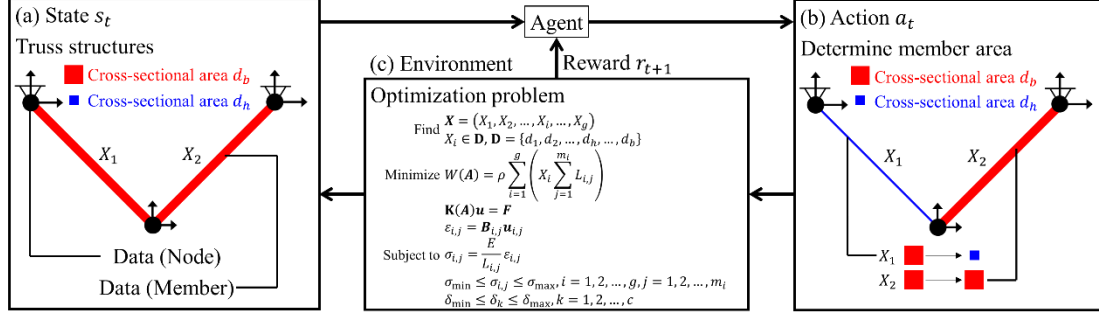


Figure 2. Proposed MDP for sizing optimization of truss structures.

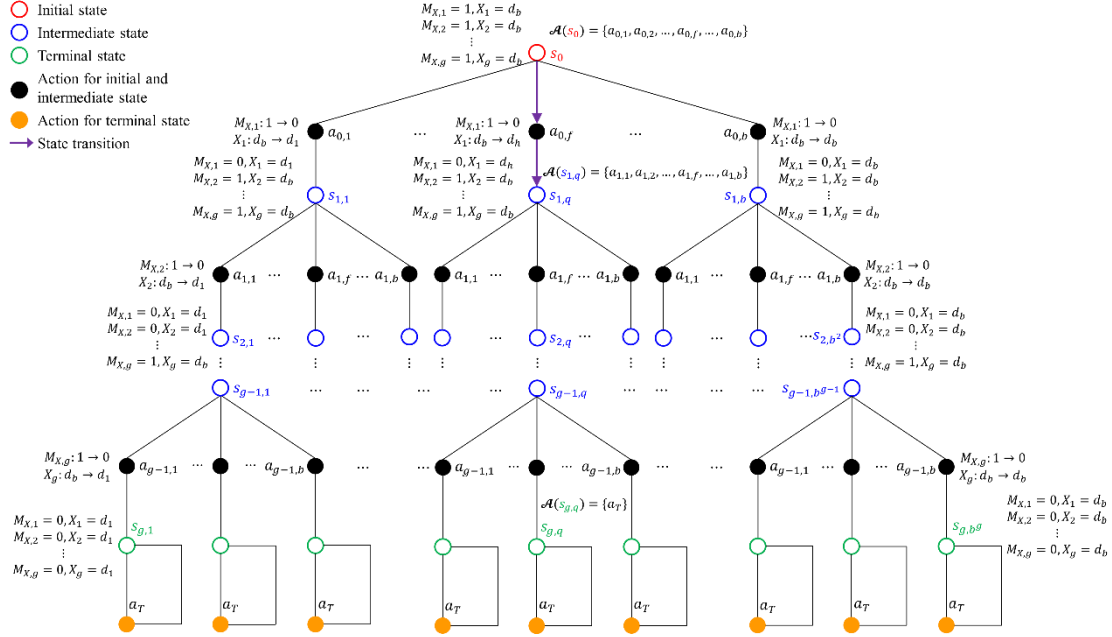


Figure 3. MDP model represented by a tree structure.

3.1.1. State

Numerical data of a truss structure is suitable for describing the state. Therefore, a state is expressed as a set of numerical data of nodes $\hat{\mathbf{v}} = \{\mathbf{v}_1, \mathbf{v}_2, \dots, \mathbf{v}_k, \dots, \mathbf{v}_c\}$ and that of members $\hat{\mathbf{w}} = \{\mathbf{w}_{1,1}, \mathbf{w}_{1,2}, \dots, \mathbf{w}_{i,j}, \dots, \mathbf{w}_{g,m_g}\}$.

(1) Node feature vector

The necessary node features include the nodal coordinates, the applied forces, and the reaction forces. Therefore, the feature vector of node k is constructed as follows:

$$\mathbf{v}_k = (x_k, y_k, z_k, F_k^x, F_k^y, F_k^z, R_k^x, R_k^y, R_k^z) \quad (3)$$

where x_k , y_k , and z_k are the coordinates of node k in the x , y , and z directions, respectively; F_k^x , F_k^y , and F_k^z are the x , y , and z components of applied force acting on node k ; and R_k^x , R_k^y , and R_k^z are the x , y , and z components of reaction force applied to

node k .

(2) Member feature vector

The necessary member features include the node numbers of the end points of the member, length, the modulus of elasticity, index to confirm if cross-sectional area is determined, and cross-sectional area. Hence, the feature vector of the member j in the group i is represented as follows:

$$\mathbf{w}_{i,j} = (H_{i,j}^1, H_{i,j}^2, L_{i,j}, E, M_{X,i}, X_i) \quad (4)$$

where $H_{i,j}^1$ and $H_{i,j}^2$ are the node numbers of both ends of the member; and $M_{X,i}$ is used to check if cross-sectional area of the member group i is determined. $M_i^A = 1$ if X_i is not determined, and $M_i^A = 0$ otherwise.

In MDP model (Figure 3), states can be classified into three types: initial state (red circle), intermediate state (blue circle), and terminal state (green circle). Initial state means that all design variables are not determined. Only one initial state is included in MDP model. Intermediate state means that some design variables are determined, and some are not. Terminal state means that all design variables are determined. s_0 , $s_{l,q}$ ($l = 1, 2, \dots, g - 1$), and $s_{g,q}$ denote the initial state, the intermediate state, and the terminal state, respectively. l is the layer number. q is the index of state for layer l . The mathematical expressions of s_0 , $s_{l,q}$, and $s_{g,q}$ are written as follows:

$$\text{State } s_0: M_{X,1} = M_{X,2} = \dots = M_{X,g} = 1 \quad (5a)$$

$$\text{State } s_{l,q}: M_{X,1} = M_{X,2} = \dots = M_{X,i} = 0 \quad (5b)$$

$$\text{and } M_{X,i+1} = M_{X,i+2} = \dots = M_{X,g} = 1 \ (i = l)$$

$$\text{State } s_{g,q}: M_{X,1} = M_{X,2} = \dots = M_{X,g} = 0 \quad (5c)$$

3.1.2. Action

Action is defined as determination of a cross-sectional area from a permissible list. In MDP model (Figure 3), actions can be divided into two categories: $a_{l,f}$ (black circle) and a_T (orange circle). Action $a_{l,f}$ ($l = 0, 1, 2, \dots, g - 1$) for initial and intermediate state is described as follows:

$$\text{Action } a_{l,f}: M_{X,i}: 1 \rightarrow 0 \text{ and } A_i: d_b \rightarrow d_h \ (i = l + 1, f = h) \quad (6)$$

where f is the index of action for layer l . Action a_T for terminal state T means that the state is not changed when it takes the action a_T . The action spaces of s_0 , $s_{l,q}$, and $s_{g,q}$ are as follows:

$$\mathcal{A}(s_0) = \{a_{0,1}, a_{0,2}, \dots, a_{0,f}, \dots, a_{0,b}\} \quad (7a)$$

$$\mathcal{A}(s_{l,q}) = \{a_{l,1}, a_{l,2}, \dots, a_{l,f}, \dots, a_{l,b}\} \quad (7b)$$

$$\mathcal{A}(s_{g,q}) = \{a_T\} \quad (7c)$$

Based on Equations (7a) and (7b), the number of elements in $\mathcal{A}(s_0)$ and $\mathcal{A}(s_{l,q})$ is the number of available sections b .

3.1.3. Reward

Reward is evaluated only for terminal state. In other words, reward for initial and intermediate state is 0. When the truss violates stress or displacement constraints, reward of 0 is assigned. Otherwise, the reward r_T is calculated as follows:

$$r_T = (\alpha/W_T)^2 \quad (8)$$

where r_T is the reward for terminal state; α is defined as the weight of the truss with cross-sectional areas of all groups equal to the smallest element in a list \mathbf{D} , i.e., d_1 , which is called the minimum weight in this study; and W_T is the weight of the truss for terminal state. r_T is a dimensionless quantity used to minimize the weight of the truss under various structural constraints.

3.2. An introduction to improved MCTS formulation

Dynamic programming (DP) is used to find optimal action sequences given a perfect model of the environment as an MDP (Figure 4(a)). The common method for DP is based on the Bellman optimality equation. Classical DP has limited ability in RL since it requires high computational complexity when solving large-scale problems (Sutton and Barto 2018). In order to deal with such situation, MCTS that combines the precision of tree search with the generality of random sampling is proposed (Browne et al. 2012). For original method, search tree with single root node (Figure 4(b)) is asymmetrically grown toward the most promising region. However, because original method is of limited utility in structural optimization problems, an improved formulation with update process, the best reward, accelerating technique, and terminal condition is developed in this study. There are many root nodes in the search tree (Figure 4(c)). A simple flowchart outlining the improved formulation is shown in Figure 5.

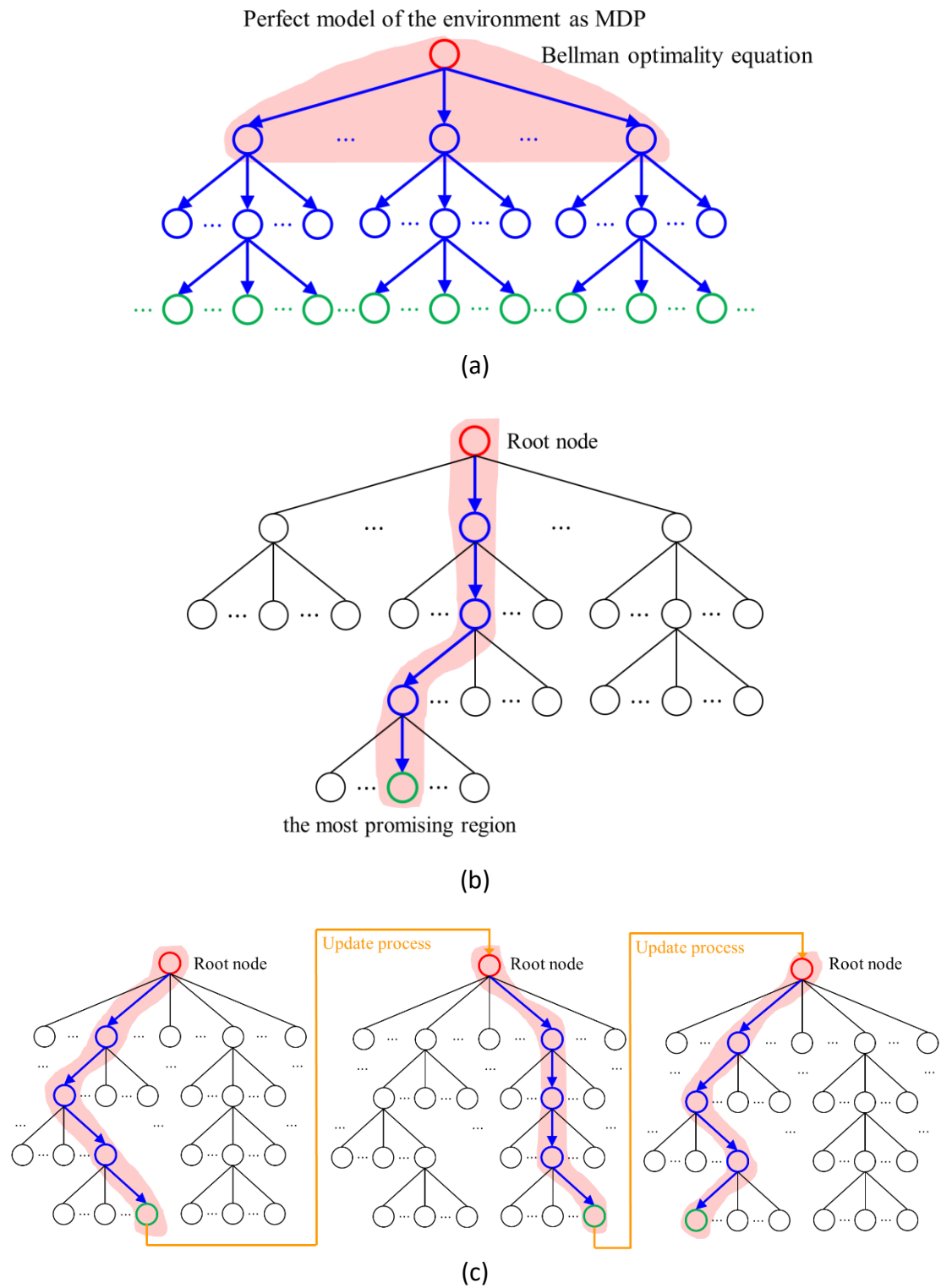


Figure 4. Tree structure for (a) DP, (b) general MCTS, and (c) improved MCTS.

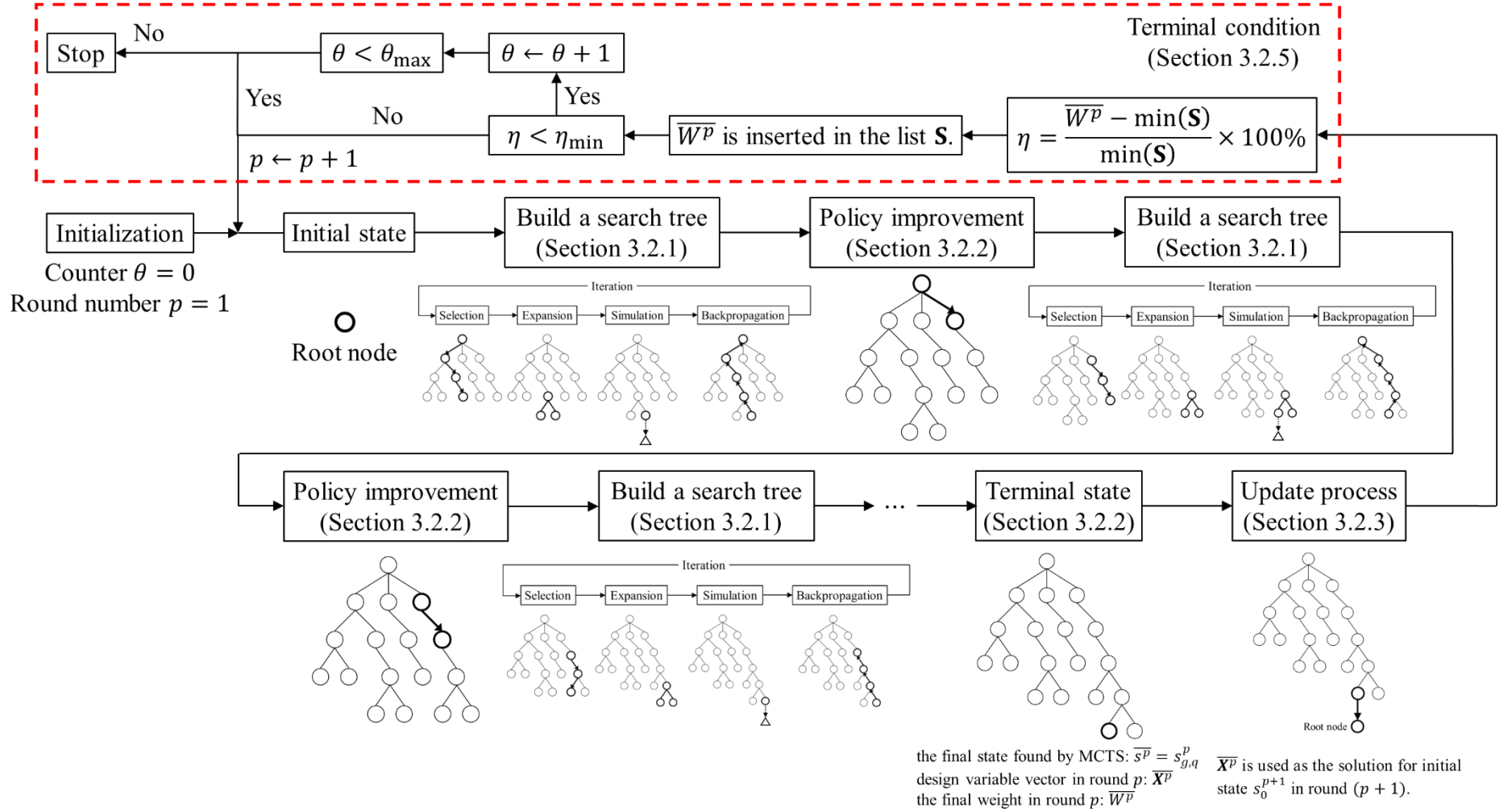


Figure 5. Flowchart of the improved MCTS formulation.

3.2.1. MCTS methodology for sizing optimization of truss structures

MCTS is a best-first search algorithm effectively applied to sizing optimization of truss structures. It utilizes a search tree to model the problem. In this study, this method builds a search tree in each round for structural optimization problems. Each node represents the state of the current truss structure. s_0^p , $s_{l,q}^p$, and $s_{g,q}^p$ denote the initial state, the intermediate state, and the final state in round p , respectively. The mathematical expressions of s_0^p , $s_{l,q}^p$, and $s_{g,q}^p$ are written as follows:

$$\text{State } s_0^p: M_{X,1}^p = M_{X,2}^p = \dots = M_{X,g}^p = 1 \quad (9a)$$

$$\text{State } s_{l,q}^p: M_{X,1}^p = M_{X,2}^p = \dots = M_{X,i}^p = 0 \quad (9b)$$

$$\text{and } M_{X,i+1}^p = M_{X,i+2}^p = \dots = M_{X,g}^p = 1 \ (i = l)$$

$$\text{State } s_{g,q}^p: M_{X,1}^p = M_{X,2}^p = \dots = M_{X,g}^p = 0 \quad (9c)$$

where $M_{X,i}^p$ is used to confirm if cross-sectional area of the member group i in round p is determined. The root node corresponds to the initial state s_0^p in round p . Nodes with terminal states $s_{g,q}^p$ are called terminal nodes. Each edge represents the action, which will be further explained in Section 3.2.3. MCTS starts with a single root node and iteratively builds a partial search tree, as shown in Figure 6. This process is repeated until reaching the predefined computational budget. The four major steps are simply summarized as follows:

- Selection: Starting at the root node, the best child node is selected recursively to descend through the tree according to a tree policy until a leaf node is reached. A leaf node contains unvisited child nodes or is a terminal node.
- Expansion: When the selected leaf node is not a terminal node, all its child nodes are added to the current tree. Then, state values and visit counts are initialized.
- Simulation: After adding the new nodes to the tree, one node is randomly chosen for simulation. Then, a simulation is run following a default policy until reaching a terminal node.
- Backpropagation: The state value and visit count are backpropagated to all nodes along the path to update the node values.

In the selection step, upper confidence bound (UCB) (Kocsis and Szepesvári 2006) is defined as follows:

$$U_n = V_n + C \sqrt{\frac{\ln J}{N_n}} \quad (10)$$

where U_n is the UCB for node n ; J is the number of iterations from root node or parent node; and C is a constant parameter to control the trade-off between exploration and exploitation. Equation (9) is used to select the best child node.

For original method, the average reward is used to update the state value in the backpropagation step (Browne et al. 2012). Because the purpose of this method is to guarantee an optimal solution path, the best reward is defined as follows:

$$V_n \leftarrow \max(V_n, G_{t_I:T}^I) \quad (11)$$

where V_n is an estimate of state value for node n through the path; $G_{t_I:T}^I$ is the return of trajectory τ_I for simulation; and I is the number of simulations. The best reward is defined as the maximum value between the current state value and the simulation result. Visit count N_n increases by 1, formulated as follows:

$$N_n \leftarrow N_n + 1 \quad (12)$$

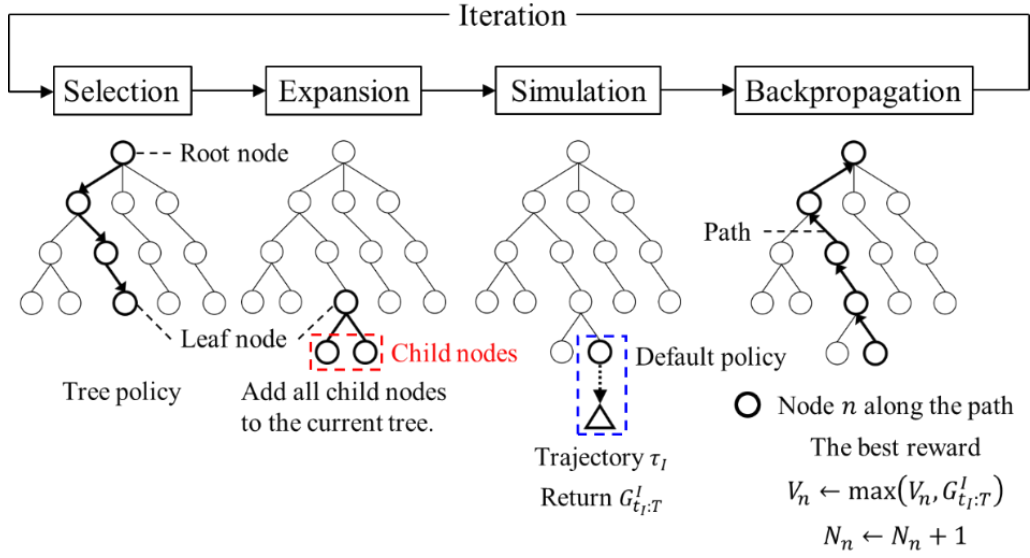


Figure 6. The four steps of the MCTS considering the best reward.

3.2.2. Policy improvement

The policy improvement process is shown in Figure 7. MCTS starts from the root node (red circle) and continues executing these four steps. After maximum number of iterations for root node is reached, a child node with the largest estimate of the state value (blue circle) is selected. This node is regarded as the parent node for the next policy improvement. Then, MCTS starts at the parent node (green circle), conducts the four steps iteratively until reaching maximum number of iterations, and the child node with the largest state value (blue circle) is chosen. After many policy improvement steps, terminal node (orange circle) is reached. The state of the terminal node is called the final state $\overline{s^p}$ in round p . The final weight $\overline{W^p}$ in round p is defined as the weight of the truss for final state.

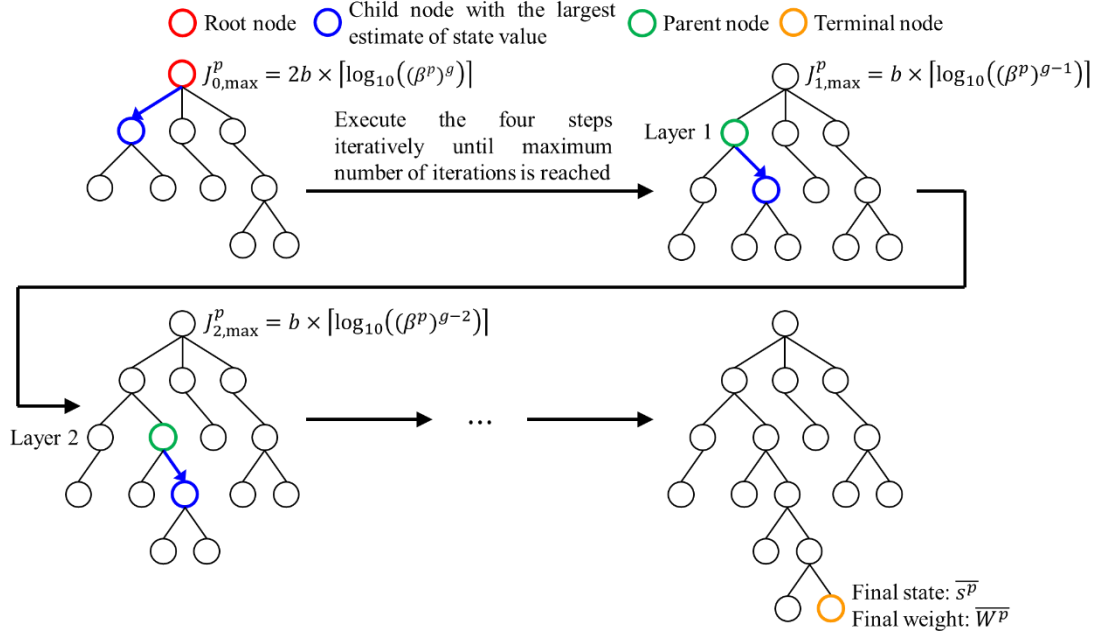


Figure 7. Policy improvement step for the MCTS.

3.2.3. Update process

For original method, there is only one root node in the search tree. It has a high possibility to trap into the local optimal solution. In order to overcome this problem, a modified version with multiple root nodes is proposed in this study. Once a final state \bar{s}^p (green circle) is found, design variable vector $\bar{\mathbf{X}}^p = (\bar{X}_1^p, \bar{X}_2^p, \dots, \bar{X}_l^p, \dots, \bar{X}_g^p)$ in round p is determined. Then, $\bar{\mathbf{X}}^p$ is used as the design variable vector $\mathbf{X}_0^{p+1} = ((X_1^{p+1})_0, (X_2^{p+1})_0, \dots, (X_l^{p+1})_0, \dots, (X_g^{p+1})_0)$ for initial state s_0^{p+1} (red circle) in round $(p + 1)$, where $(X_i^{p+1})_0$ is the cross-sectional area of the member group i . It is called an update process (orange line) in this study, as shown in Figure 8. Since the starting point of a path is the maximum value, all design variables for initial state s_0^1 in round 1 is equal to the largest element in a list \mathbf{D} , i.e., d_b . The center of the search space needs to be the design variable vector for initial state. For this purpose, a list $\mathbf{D}_i^p = \{(d_i^p)_1, \dots, (d_i^p)_h, \dots, (d_i^p)_\mu, \dots, (d_i^p)_{\beta_p}\}$ with member areas belonging to \mathbf{D} is defined (table in Figure 8), where $(d_i^p)_\mu$ is the median of the list \mathbf{D}_i^p and equal to $(X_i^p)_0$; and β^p is the number of elements in the list \mathbf{D}_i^p . When considering update process, action $a_{l,f}^p$ ($l = 0, 1, 2, \dots, g - 1$) for initial and intermediate state is described as follows:

$$\text{Action } a_{l,f}^p: M_{X,l}^p: 1 \rightarrow 0 \text{ and } X_l^p: (X_l^p)_0 \rightarrow (d_l^p)_h \text{ (} i = l + 1, f = h \text{)} \quad (13)$$

where X_l^p is the cross-sectional area of the member group i in round p . The action spaces of s_0^p and $s_{l,q}^p$ are as follows:

$$\mathcal{A}(s_0^p) = \{a_{0,1}^p, a_{0,2}^p, \dots, a_{0,f}^p, \dots, a_{0,\beta^p}^p\} \quad (14a)$$

$$\mathcal{A}(s_{l,q}^p) = \{a_{l,1}^p, a_{l,2}^p, \dots, a_{l,f}^p, \dots, a_{l,\beta^p}^p\} \quad (14b)$$

Based on Equations (14a) and (14b), the number of elements in $\mathcal{A}(s_0^p)$ and $\mathcal{A}(s_l^p)$ is equal to β^p .

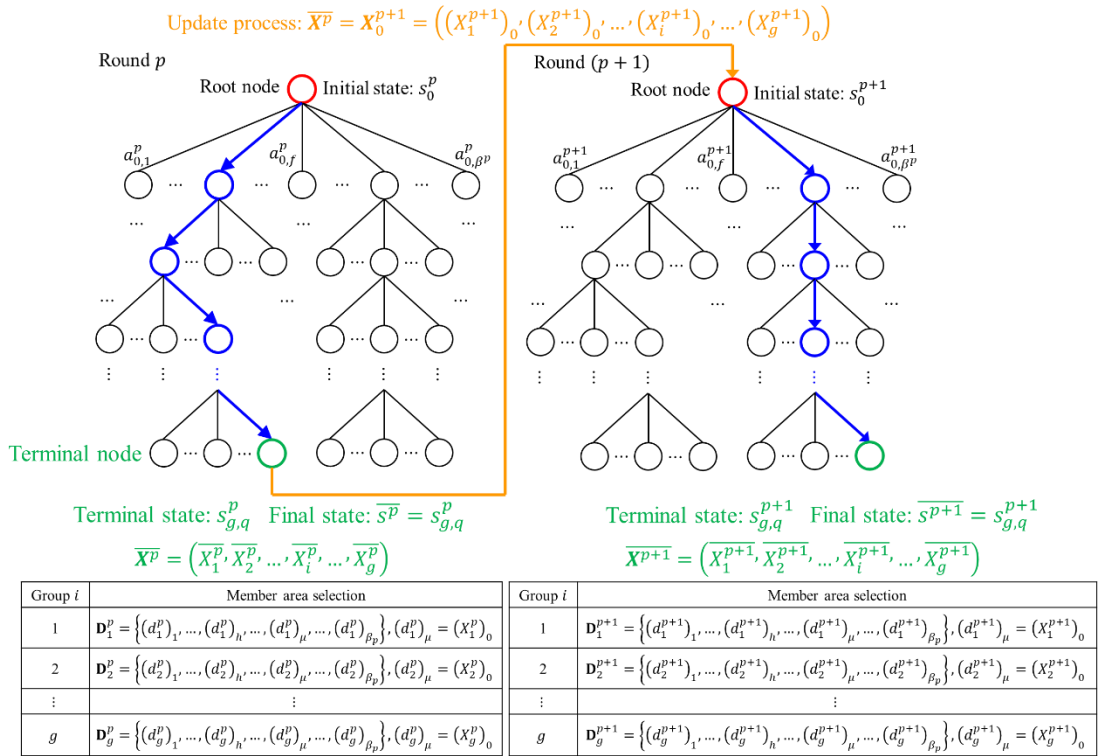


Figure 8. Update process for sizing optimization of truss structures.

3.2.4. Accelerating technique

In this study, accelerating technique is developed by decreasing the width of search tree during the update process (Figure 9). β^p is formulated as follows:

$$\beta^1 = \begin{cases} b & \text{if } b \text{ is odd number} \\ b + 1 & \text{if } b \text{ is even number} \end{cases} \quad (15a)$$

$$\varphi^p = \beta^1 \times 0.5^{\left\lceil \frac{p-1}{r} \right\rceil} \quad (15b)$$

$$\phi^p = \lfloor \varphi^p \rfloor \quad (15c)$$

$$\omega^p = \begin{cases} \phi^p & \text{if } \phi^p \text{ is odd number} \\ \phi^p + 1 & \text{if } \phi^p \text{ is even number} \end{cases} \quad (15d)$$

$$\beta^p = \max(3, \omega^p) \quad (15e)$$

Equation (15a) indicates that β^1 is based on the number of available variables b . In order to reduce the computational time, β^p is decreasing geometrically when more and more round is reached. For this reason, Equation (15b) is used to satisfy this requirement, where $\lceil \frac{p-1}{\gamma} \rceil$ is the least integer greater than or equal to $\frac{p-1}{\gamma}$; and γ is a constant parameter to decrease β^p geometrically, which is set to 3 in this study. Equation (15c) is used to ensure that β^p is an integer, where $\lfloor \varphi^p \rfloor$ is the greatest integer less than or equal to φ^p . Equation (15e) is adopted because the minimum value of β^p needs to be 3, where $\max(3, \beta^p)$ is the largest value between 3 and β^p . The number of elements on the left and right side of $(d_i^p)_\mu$ needs to be the same since the same possibility of searching both directions is necessary. Therefore, Equation (15a) and Equation (15d) is used to ensure that β^p is the odd number.

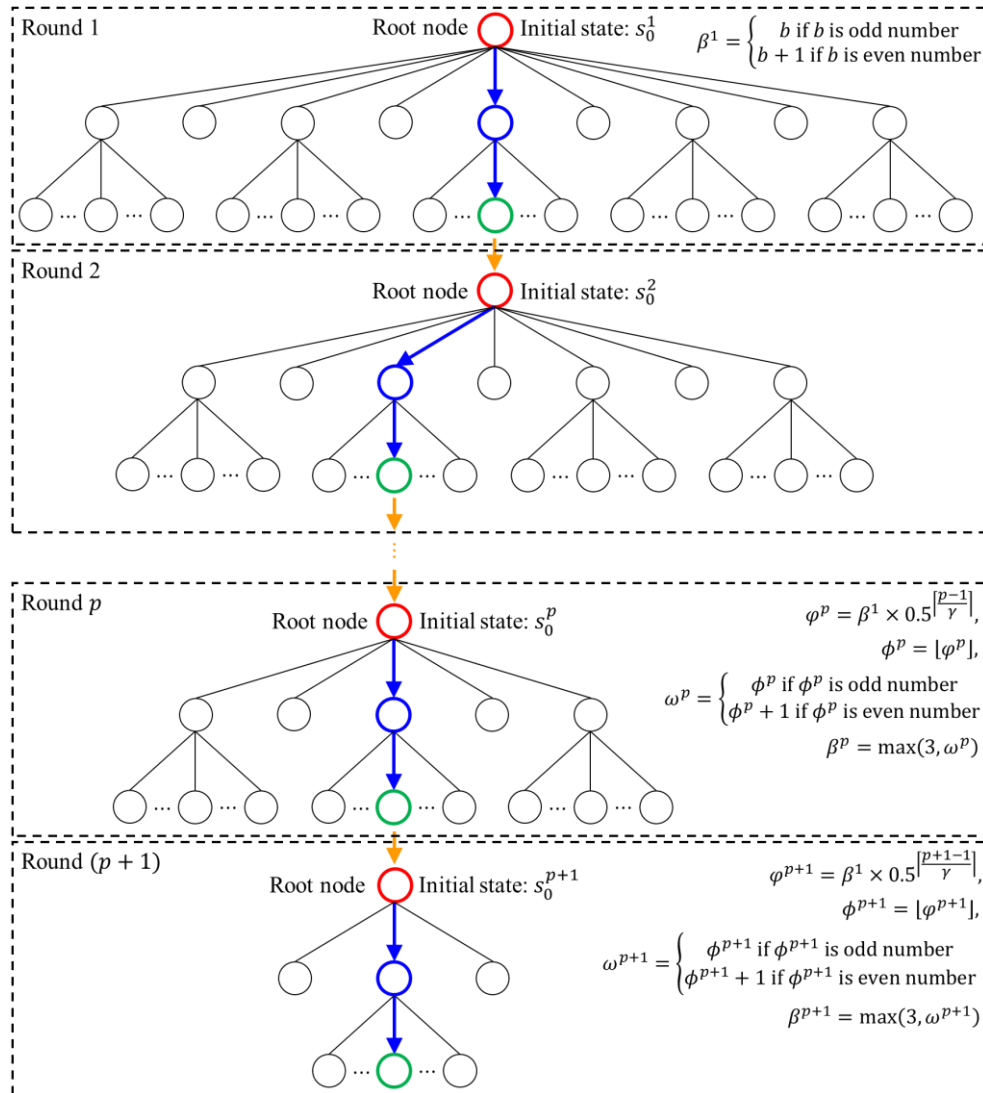


Figure 9. Accelerating technique for modified version of MCTS.

When performing more and more policy improvement steps, maximum number of iterations needs to be decrease geometrically. Hence, maximum number of iterations for root node $J_{0,\max}^p$ and parent node $J_{l,\max}^p$ for layer l ($l = 1, 2, \dots, g - 1$) (Figure 7) is expressed as follows:

$$\text{For root node (initial state)} \quad J_{0,\max}^p = 2b \times \lceil \log_{10}((\beta^p)^g) \rceil \quad (16a)$$

$$\text{For parent node (intermediate state)} \quad J_{l,\max}^p = b \times \lceil \log_{10}((\beta^p)^{g-l}) \rceil \quad (16b)$$

3.2.5. Terminal condition

Update process (Section 3.2.3) is carried out multiple rounds until the terminal condition is satisfied. For terminal condition, a list \mathbf{S} is defined to store the final weight \overline{W}^p in round p . \overline{W}^0 is defined as the weight of the truss with all design variables set to d_b , which is called the maximum weight in this study. Improvement factor η and counter θ are defined to ensure convergence of the algorithm. The improvement factor is defined as follows:

$$\eta = |(\overline{W}^p - \min(\mathbf{S})) / \min(\mathbf{S}) \times 100\%| \quad (17)$$

where $\min(\mathbf{S})$ is the smallest element in a list \mathbf{S} . Before execution of an algorithm, \overline{W}^0 is in a list \mathbf{S} , and θ is set to 0. At the end of the round, the improvement factor η is calculated, and then \overline{W}^p is inserted in a list \mathbf{S} . When $\eta < \eta_{\min}$, θ is set to $\theta + 1$. If $\theta \geq \theta_{\max}$, the algorithm terminates. η_{\min} and θ_{\max} are the critical value of improvement factor and the maximum number of counters for termination, respectively. In this study, η_{\min} and θ_{\max} are set to 0.01% and 3. At this time, $\min(\mathbf{S})$ is the optimal solution of the optimization problem in Section 2. The flowchart of the terminal condition is shown in Figure 10.

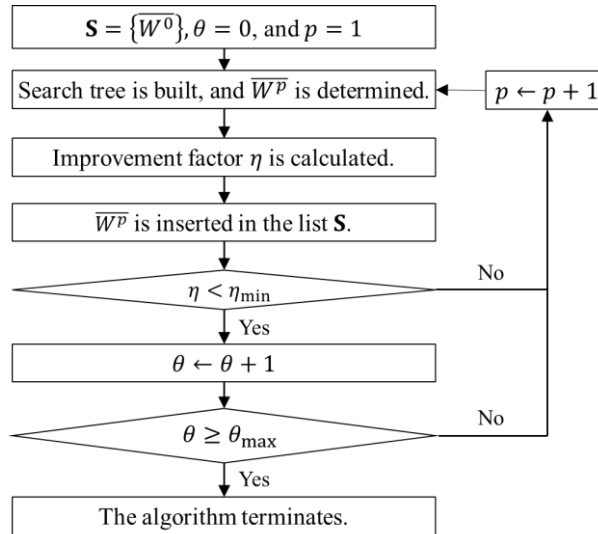


Figure 10. Terminal condition for improved MCTS formulation.

4. Numerical examples with discrete design variables

In this section, three truss optimization problems are examined to show the effectiveness of the proposed method. At first, 10-bar planar truss and 72-bar spatial truss which have been previously studied by other investigators are used to investigate the numerical correctness. Then, 220-bar transmission tower is used to show that this method is suitable for practical engineering problems. This algorithm and the direct stiffness method for the analysis of truss structures are coded in Python programming software. The computations are carried out with Intel Core i7 2.30 GHz processor and 40 GB memory.

4.1. Problem description

Figure 11 demonstrates the 10-bar planar truss, previously being analyzed by many metaheuristic algorithms, such as genetic algorithm (GA) (Rajeev and Krishnamoorthy 1992), ant colony optimization (ACO) (Camp and Bichon 2004), particle swarm optimizer (PSO) (Li, Huang, and Liu 2009), artificial bee colony (ABC) algorithm (Sonmez 2011), mine blast algorithm (MBA) (Sadollah et al. 2012), water cycle algorithm (WCA) (Eskandar, Sadollah, and Bahreininejad 2013), subset simulation algorithm (SSA) (Li and Ma 2015), and artificial coronary circulation system (ACCS) (Kooshkbaghi, Kaveh, and Zarfam 2020). Various design parameters considered here are shown in Tables 1-3.

A 72-bar spatial truss is shown in Figure 12, which has been investigated by many methods, such as GA (Wu and Chow 1995), harmony search (HS) (Lee et al. 2005), PSO (Li, Huang, and Liu 2009), MBA (Sadollah et al. 2012), SSA (Li and Ma 2015), ACCS (Kooshkbaghi, Kaveh, and Zarfam 2020). For analysis, various design parameters are captured from Tables 1-3.

The 220-bar transmission tower is shown in Figure 13. Similarly, like the previous cases for analysis purpose, various design parameters are taken from Tables 1-3.

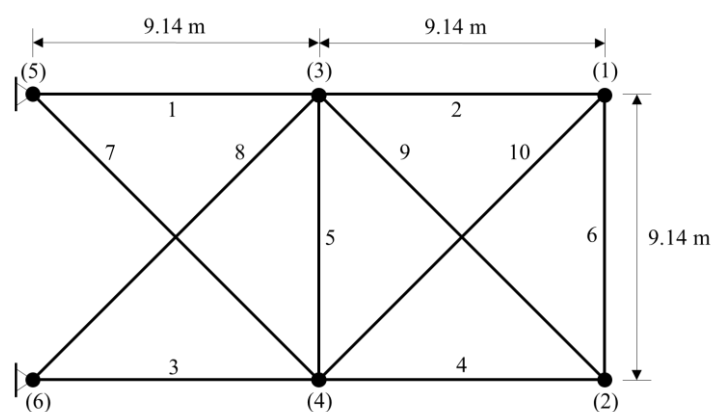


Figure 11. A 10-bar planar truss.

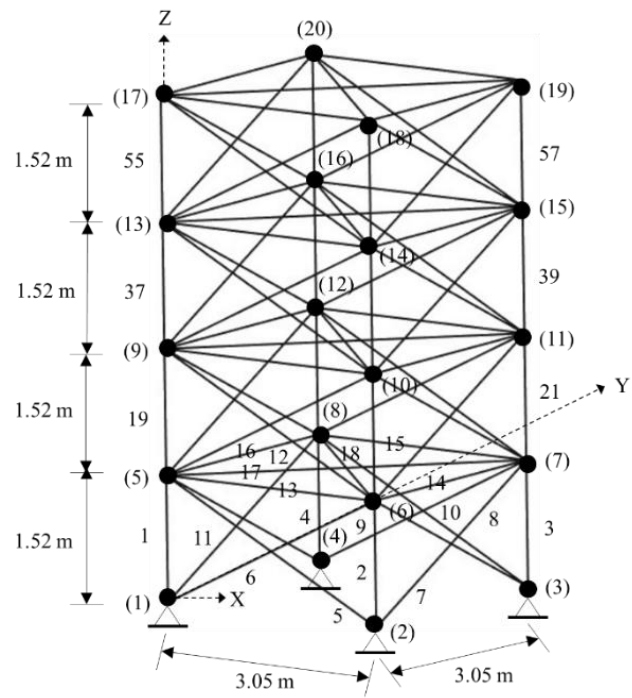


Figure 12. A 72-bar spatial truss.

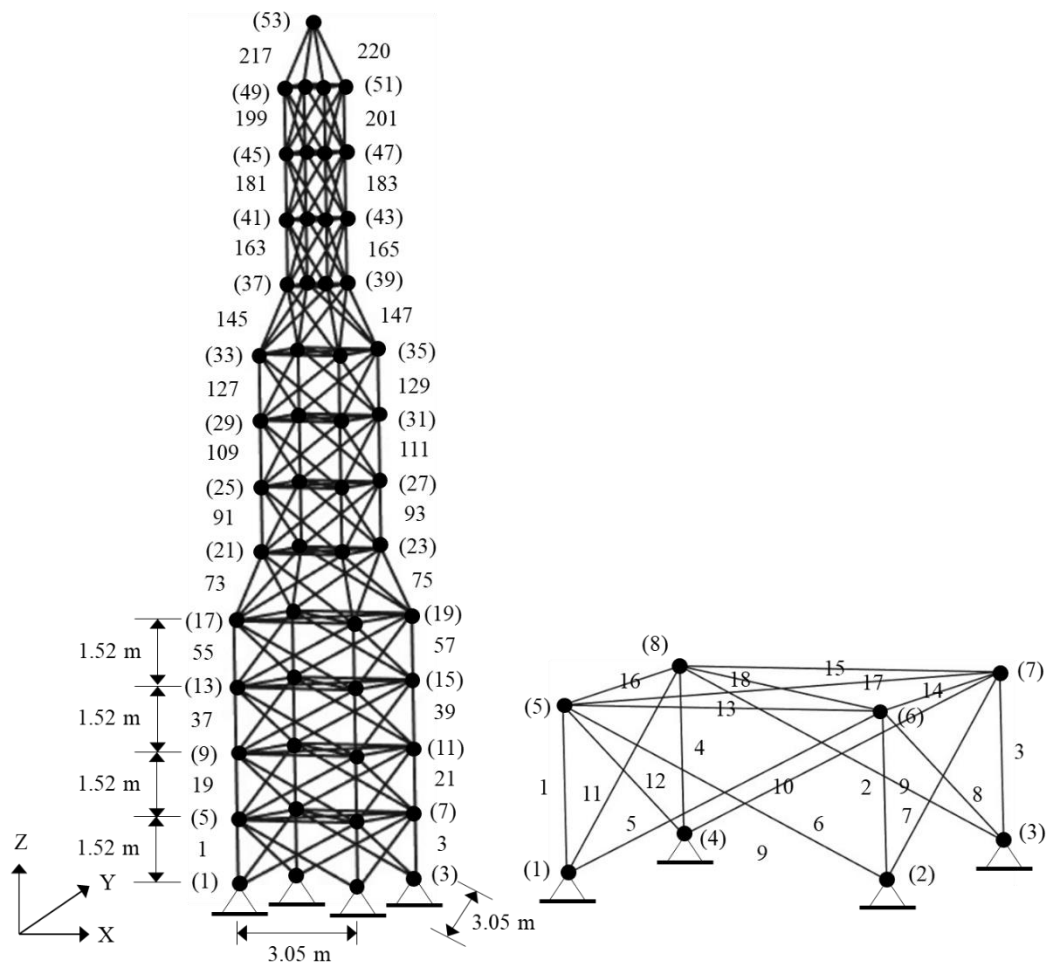


Figure 13. A 220-bar transmission tower.

Table 1. Design consideration of the truss optimization problems.

	10-bar planar truss	72-bar spatial truss	220-bar transmission tower
Design variables	$A_i, i = 1, 2, \dots, 10$	$A_i, i = 1, 2, \dots, 16$	$A_i, i = 1, 2, \dots, 49$
Material density (kg/m ³)	2767.99	2767.99	7860.00
Modulus of elasticity (GPa)	68.95	68.95	207.00
Stress limitation (MPa)	± 172.37	± 172.37	± 180.00
Displacement limitation (mm)	± 50.80	± 6.35	± 6.35
Load (kN)	$P_2^Y = P_4^Y = 444.82$	Table 4	Table 5

Table 2. Member group of the truss optimization problems.

Truss problems	Discrete set
10-bar planar truss	No member group
72-bar spatial truss	72 truss members grouped into 16 design variables, as follows: (1) A_1-A_4 , (2) A_5-A_{12} , (3) $A_{13}-A_{16}$, (4) $A_{17}-A_{18}$, (5) $A_{19}-A_{22}$, (6) $A_{23}-A_{30}$, (7) $A_{31}-A_{34}$, (8) $A_{35}-A_{36}$, (9) $A_{37}-A_{40}$, (10) $A_{41}-A_{48}$, (11) $A_{49}-A_{52}$, (12) $A_{53}-A_{54}$, (13) $A_{55}-A_{58}$, (14) $A_{59}-A_{66}$, (15) $A_{67}-A_{70}$, and (16) $A_{71}-A_{72}$
220-bar transmission tower	Table 6

Table 3. Discrete set of the truss optimization problems.

Truss problems	Discrete set
10-bar planar truss	Case 1: $\mathbf{D} = \{1045.16, 1161.29, 1283.87, 1374.19, 1535.48, 1690.32, 1696.77, 1858.06, 1890.32, 1993.54, 2019.35, 2180.64, 2238.71, 2290.32, 2341.93, 2477.41, 2496.77, 2503.22, 2696.77, 2722.58, 2896.77, 2961.28, 3096.77, 3206.45, 3303.22, 3703.22, 4658.06, 5141.93, 7419.34, 8709.66, 8967.72, 9161.27, 9999.98, 10322.56, 10903.20, 12129.01, 12838.68, 14193.52, 14774.16, 17096.74, 19354.80, 21612.86\}$ mm ² Case 2: $\mathbf{D} = \{64.52, 322.60, 645.20 \dots 19678.60, 20001.20, 20323.80\}$ mm ²
72-bar spatial truss	Case 1: $\mathbf{D} = \{64.50, 129.00, 193.50 \dots 1935.00, 1999.50, 2064.00\}$ mm ² Case 2: American Institute of Steel Construction (AISC) (Table 7)
220-bar transmission tower	AISC (Table 7)

Table 4. Load cases for the 72-bar spatial truss.

Nodes k	Load case 1 (kN)			Load case 2 (kN)		
	P_k^X	P_k^Y	P_k^Z	P_k^X	P_k^Y	P_k^Z
17	22.24	22.24	-22.24	0.00	0.00	-22.24
18	0.00	0.00	0.00	0.00	0.00	-22.24
19	0.00	0.00	0.00	0.00	0.00	-22.24
20	0.00	0.00	0.00	0.00	0.00	-22.24

Table 5. Load cases for the 220-bar transmission tower.

Nodes k	Load case 1 (kN)			Load case 2 (kN)		
	P_k^X	P_k^Y	P_k^Z	P_k^X	P_k^Y	P_k^Z
49	0.00	0.00	0.00	0.00	0.00	-400.00
50	0.00	0.00	0.00	0.00	0.00	-400.00
51	0.00	0.00	0.00	0.00	0.00	-400.00
52	0.00	0.00	0.00	0.00	0.00	-400.00
53	0.00	0.00	-2000.00	0.00	0.00	-400.00

Table 6. Member group for the 220-bar transmission tower.

Number	Members	Number	Members	Number	Members	Number	Members
1	1–4	14	59–66	27	121–124	40	179–180
2	5–12	15	67–70	28	125–126	41	181–184
3	13–16	16	71–72	29	127–130	42	185–192
4	17–18	17	73–76	30	131–138	43	193–196
5	19–22	18	77–84	31	139–142	44	197–198
6	23–30	19	85–88	32	143–144	45	199–202
7	31–34	20	89–90	33	145–148	46	203–210
8	35–36	21	91–94	34	149–156	47	211–214
9	37–40	22	95–102	35	157–160	48	215–216
10	41–48	23	103–106	36	161–162	49	217–220
11	49–52	24	107–108	37	163–166		
12	53–54	25	109–112	38	167–174		
13	55–58	26	113–120	39	175–178		

Table 7. Discrete values available for cross-sectional areas from AISC norm.

Number	Area (mm ²)	Number	Area (mm ²)	Number	Area (mm ²)	Number	Area (mm ²)
1	71.61	17	1008.39	33	2477.41	49	7419.34
2	90.97	18	1045.16	34	2496.77	50	8709.66
3	126.45	19	1161.29	35	2503.22	51	8967.72
4	161.29	20	1283.87	36	2696.77	52	9161.27
5	198.06	21	1374.19	37	2722.58	53	9999.98
6	252.26	22	1535.48	38	2896.77	54	10322.56
7	285.16	23	1690.32	39	2961.28	55	10903.20
8	363.23	24	1696.77	40	3096.77	56	12129.01
9	388.39	25	1858.06	41	3206.45	57	12838.68
10	494.19	26	1890.32	42	3303.22	58	14193.52
11	506.45	27	1993.54	43	3703.22	59	14774.16
12	641.29	28	2019.35	44	4658.06	60	15806.42
13	645.16	29	2180.64	45	5141.93	61	17096.74
14	792.26	30	2238.71	46	5503.22	62	18064.48
15	816.77	31	2290.32	47	5999.99	63	19354.80
16	940.00	32	2341.93	48	6999.99	64	21612.86

4.2. Investigation of convergence history: 10-bar planar truss

Figure 14 illustrates the comparison of convergence histories for the 10-bar planar truss under the best and average reward. Figures 14(a) and 14(b) for Case 1 and Case 2 demonstrate that the proposed method obtains the best solution at 13 and 15 rounds under the best reward. However, this method does not detect the best solution after 40 rounds under the average reward.

The comparison of convergence histories for the 10-bar planar truss under different parameter α is shown in Figure 15. From Figures 15(a) and 15(b), this algorithm obtains the best solution at 13 and 18 rounds under minimum weight for Case 1 and Case 2. However, for Case 1 and Case 2, this algorithm does not detect the best solution after 40 rounds under maximum weight.

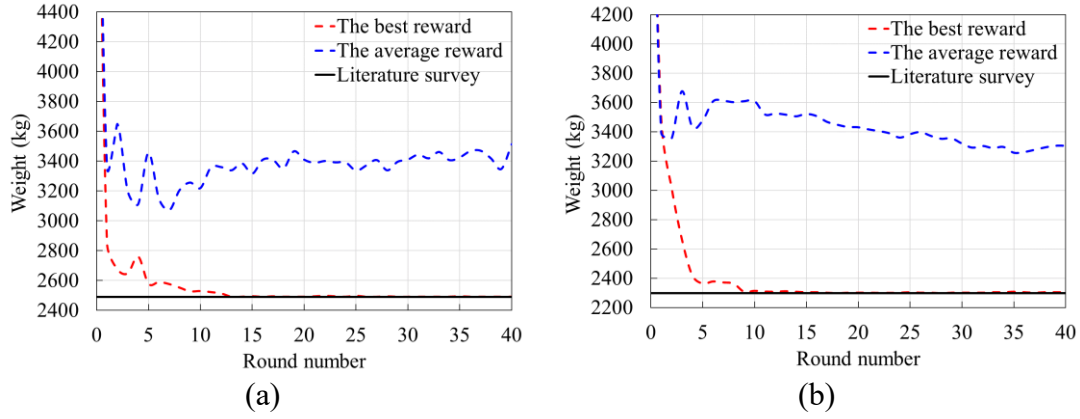


Figure 14. Comparison of the convergence histories for 10-bar planar truss under the best and average reward for (a) Case 1 and (b) Case 2.

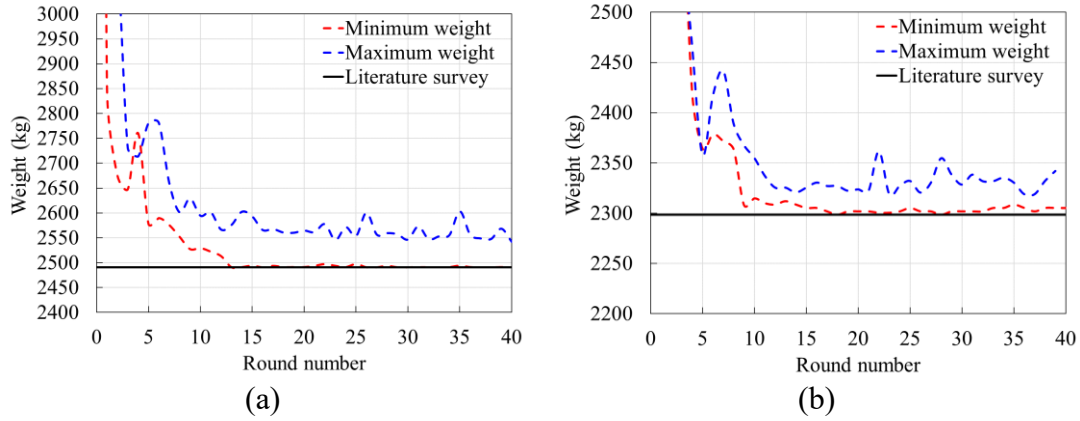


Figure 15. Comparison of the convergence histories for 10-bar planar truss under parameter α equal to minimum and maximum weight for (a) Case 1 and (b) Case 2.

4.3. Comparison of original and modified version of MCTS formulation

Table 8 presents the comparison of original and modified version for the 10-bar planar truss and 72-bar spatial truss. From Table 8, it can be seen that modified version can find the optimal solution. However, the solution found by original version can trap into the local optimum.

Table 8. Optimal solution found by original and modified version of MCTS.

Investigated example	Best weight	Worst weight	Average weight	Standard deviation
10-bar planar truss (Case 1)	2490.56 kg	2523.38 kg	2500.94 kg	11.81
10-bar planar truss (Case 2)	2298.50 kg	2308.07 kg	2303.26 kg	3.15
72-bar spatial truss (Case 1)	174.88 kg	177.06 kg	176.07 kg	0.60
72-bar spatial truss (Case 2)	176.60 kg	179.47 kg	176.94 kg	0.89
220-bar transmission tower	6991.00 kg	7193.25 kg	7091.14 kg	64.73

4.4. Solution accuracy

Tables 9-12 compare the optimal designs of this method with other algorithms from the literature. It is clear that this method has the ability to provide the best solution (lightest weight) compared with other algorithms. Table 13 is the optimal design for 220-bar transmission tower. Figures 16-20 reveal that the optimal solution assessed by this approach does not violate stress and displacement constraints. The results demonstrate that this method is suitable for both benchmark and practical engineering problems.

Table 9. Comparison of optimum designs for the 10-bar planar truss (Case 1).

Variables		Optimal cross-sectional areas (mm ²)					
No	Design Variables	GA	ACO	PSO	ABC	ACCS	This study
1	A_1	21612.86	21612.86	19354.80	21612.86	21612.86	21612.86
2	A_2	1045.16	1045.16	1045.16	1045.16	1045.16	1045.16
3	A_3	14193.52	14774.16	19354.80	14774.16	14774.16	14774.16
4	A_4	9999.98	9161.27	8709.66	9161.27	9161.27	9161.27
5	A_5	1045.16	1045.16	1045.16	1045.16	1045.16	1045.16
6	A_6	1045.16	1045.16	1161.29	1045.16	1045.16	1045.16
7	A_7	9161.27	5141.93	7419.34	5141.93	5141.93	5141.93
8	A_8	12838.68	14774.16	12129.01	14774.16	14774.16	14774.16
9	A_9	12838.68	14193.52	14193.52	14193.52	14193.52	14193.52
10	A_{10}	1690.32	1045.16	1161.29	1045.16	1045.16	1045.16
Optimal weight (kg)		2546.39	2490.56	2531.84	2490.56	2490.56	2490.56

Table 10. Comparison of optimum designs for the 10-bar planar truss (Case 2).

Variables		Optimal cross-sectional areas (mm ²)					
No	Design Variables	PSO	MBA	WCA	SSA	ACCS	This study
1	A_1	15807.40	19033.40	19356.00	19356.00	19678.60	19678.60
2	A_2	64.52	64.52	64.52	64.52	64.52	64.52
3	A_3	14517.00	15484.80	15162.20	15162.20	14839.60	15162.20
4	A_4	10000.60	9678.00	9678.00	9678.00	9678.00	9355.40
5	A_5	64.52	64.52	64.52	64.52	64.52	64.52
6	A_6	967.80	322.60	322.60	322.60	322.60	322.60
7	A_7	5484.20	4839.00	4839.00	4839.00	4839.00	4839.00
8	A_8	13871.80	13871.80	13871.80	13871.80	13549.20	13549.20
9	A_9	17743.00	13871.80	13871.80	13871.80	14194.40	14194.40
10	A_{10}	64.52	64.52	64.52	64.52	64.52	64.52
Optimal weight (kg)		2378.51	2298.50	2298.50	2298.50	2298.50	2298.50

Table 11. Comparison of optimum designs for the 72-bar spatial truss (Case 1).

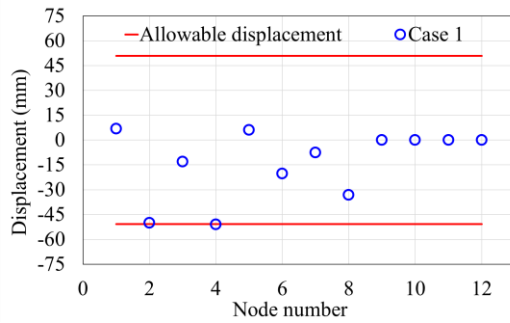
Variables		Optimal cross-sectional areas (mm ²)					
No	Design Variables	GA	HS	PSO	MBA	ACCS	This study
1	$A_1 - A_4$	967.50	1225.50	1677.00	1290.00	1290.00	1290.00
2	$A_5 - A_{12}$	451.50	322.50	967.50	387.00	322.50	322.50
3	$A_{13} - A_{16}$	64.50	64.50	193.50	258.00	64.50	64.50
4	$A_{17} - A_{18}$	64.50	64.50	64.50	387.00	64.50	64.50
5	$A_{19} - A_{22}$	838.50	903.00	1354.50	322.50	838.50	838.50
6	$A_{23} - A_{30}$	322.50	387.00	967.50	322.50	322.50	322.50
7	$A_{31} - A_{34}$	129.00	64.50	387.00	64.50	64.50	64.50
8	$A_{35} - A_{36}$	64.50	64.50	193.50	64.50	64.50	64.50
9	$A_{37} - A_{40}$	322.50	387.00	1419.00	903.00	322.50	322.50
10	$A_{41} - A_{48}$	322.50	322.50	1225.50	322.50	322.50	322.50
11	$A_{49} - A_{52}$	64.50	64.50	129.00	64.50	64.50	64.50
12	$A_{53} - A_{54}$	129.00	64.50	580.50	64.50	64.50	64.50
13	$A_{55} - A_{58}$	129.00	129.00	258.00	1225.50	129.00	129.00
14	$A_{59} - A_{66}$	322.50	322.50	1225.50	322.50	387.00	387.00
15	$A_{67} - A_{70}$	322.50	258.00	451.50	64.50	258.00	258.00
16	$A_{71} - A_{72}$	451.50	387.00	1032.00	64.50	387.00	387.00
Optimal weight (kg)		181.74	175.97	494.36	174.88	174.88	174.88

Table 12. Comparison of optimum designs for the 72-bar spatial truss (Case 2).

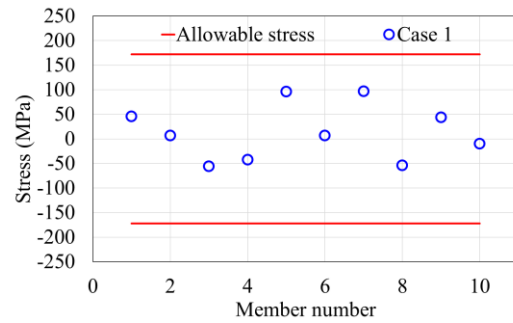
Variables		Optimal cross-sectional areas (mm ²)					
No	Design Variables	GA	PSO	MBA	SSA	ACCS	This study
1	$A_1 - A_4$	126.45	4658.06	126.45	1283.87	1283.87	1283.87
2	$A_5 - A_{12}$	388.39	1161.29	363.23	363.23	285.16	363.23
3	$A_{13} - A_{16}$	198.06	729.03	285.16	71.61	71.61	71.61
4	$A_{17} - A_{18}$	494.19	126.45	388.39	71.61	71.61	71.61
5	$A_{19} - A_{22}$	252.26	1993.54	285.16	792.26	792.26	792.26
6	$A_{23} - A_{30}$	252.26	506.45	285.16	363.23	363.23	285.16
7	$A_{31} - A_{34}$	90.97	363.23	71.61	71.61	71.61	71.61
8	$A_{35} - A_{36}$	71.61	506.45	71.61	71.61	71.61	71.61
9	$A_{37} - A_{40}$	1161.29	1993.54	816.77	363.23	363.23	363.23
10	$A_{41} - A_{48}$	388.39	792.26	363.23	285.16	363.23	363.23
11	$A_{49} - A_{52}$	90.97	71.61	71.61	71.61	71.61	71.61
12	$A_{53} - A_{54}$	198.06	363.23	71.61	71.61	71.61	71.61
13	$A_{55} - A_{58}$	1008.39	1283.87	1161.29	126.45	126.45	126.45
14	$A_{59} - A_{66}$	494.19	1045.16	388.39	363.23	363.23	363.23
15	$A_{67} - A_{70}$	90.97	1008.39	71.61	252.26	252.26	252.26
16	$A_{71} - A_{72}$	71.61	816.77	71.61	363.23	363.23	363.23
Optimal weight (kg)		193.78	548.61	177.23	176.60	176.60	176.60

Table 13. Optimal design for 220-bar transmission tower.

Number	Area (mm ²)	Number	Area (mm ²)	Number	Area (mm ²)	Number	Area (mm ²)
1	8967.72	14	71.61	27	90.97	40	363.23
2	71.61	15	2238.71	28	506.45	41	8967.24
3	71.61	16	1008.39	29	9161.27	42	71.61
4	71.61	17	9999.98	30	71.61	43	71.61
5	8967.72	18	71.61	31	2290.32	44	71.61
6	71.61	19	1535.48	32	1008.39	45	9161.27
7	71.61	20	2496.77	33	10322.56	46	71.61
8	71.61	21	9161.27	34	71.61	47	1535.48
9	8709.66	22	71.61	35	645.16	48	1690.32
10	71.61	23	90.97	36	2961.28	49	10322.56
11	71.61	24	161.29	37	8967.24		
12	71.61	25	9161.27	38	90.97		
13	8967.72	26	90.97	39	71.61		

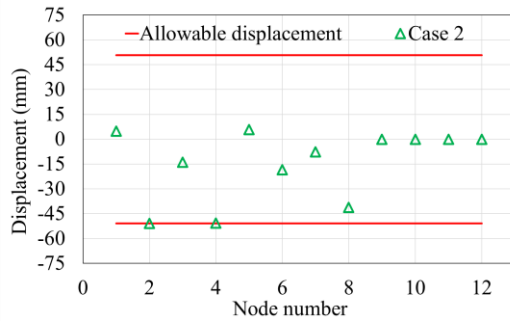


(a)

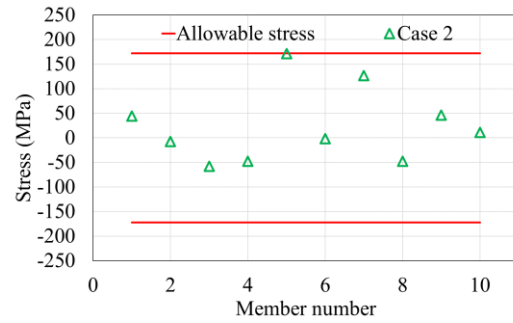


(b)

Figure 16. Constraints evaluated at the optimal design of 10-bar planar truss (Case 1) by this method for (a) displacement constraints and (b) stress constraints.



(a)



(b)

Figure 17. Constraints evaluated at the optimal design of 10-bar planar truss (Case 2) by this method for (a) displacement constraints and (b) stress constraints.

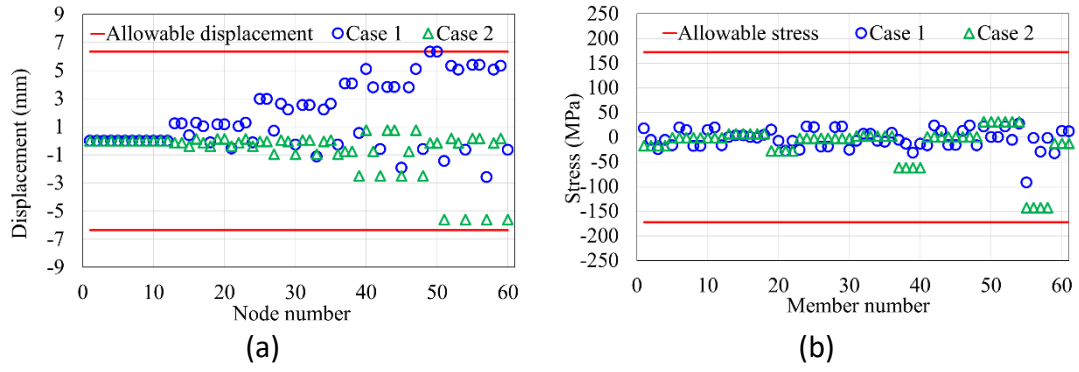


Figure 18. Constraints evaluated at the optimal design of 72-bar spatial truss (Case 1) by this method for (a) displacement constraints and (b) stress constraints.

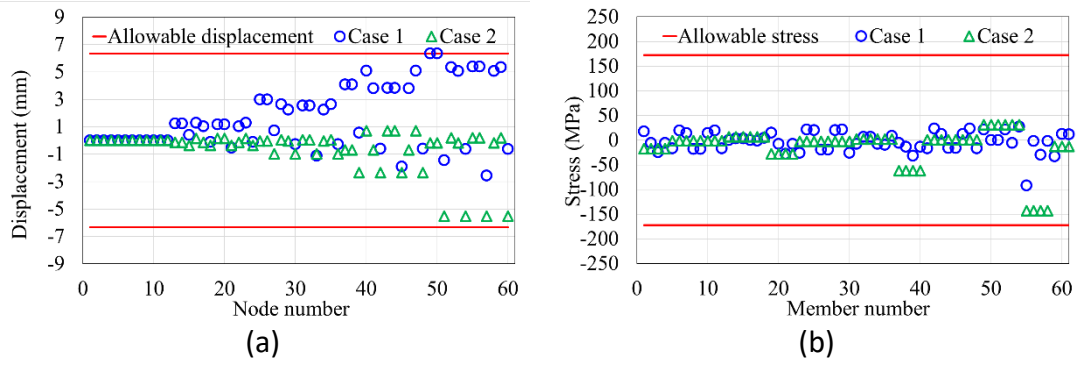


Figure 19. Constraints evaluated at the optimal design of 72-bar spatial truss (Case 2) by this method for (a) displacement constraints and (b) stress constraints.

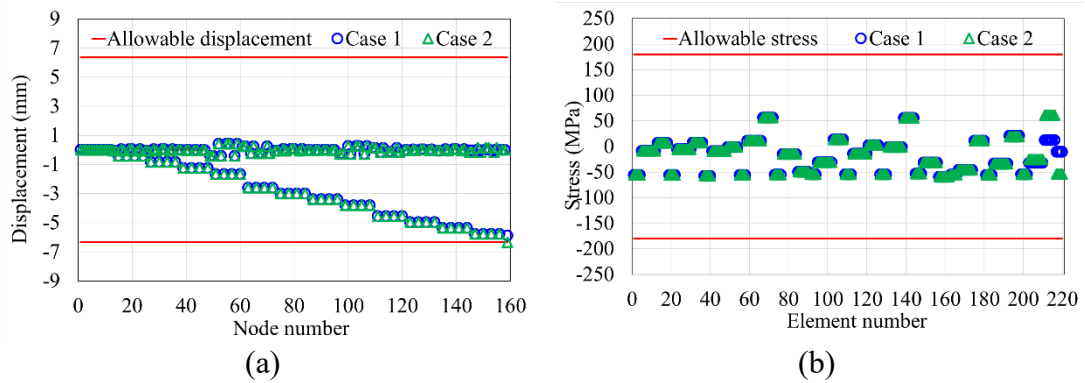


Figure 20. Constraints evaluated at the optimal design of 220-bar transmission tower by this method for (a) displacement constraints and (b) stress constraints.

4.5. Solution stability

The statistical results of all truss optimization problems are obtained through 10 independent sampling to test the stability of this method. The results are summarized in Table 14, including the best, the worst, average, and standard deviation.

Table 14. Statistical results of the investigated example.

Investigated example	Best weight	Worst weight	Average weight	Standard deviation
10-bar planar truss (Case 1)	2490.56 kg	2523.38 kg	2500.94 kg	11.81
10-bar planar truss (Case 2)	2298.50 kg	2308.07 kg	2303.26 kg	3.15
72-bar spatial truss (Case 1)	174.88 kg	177.06 kg	176.07 kg	0.60
72-bar spatial truss (Case 2)	176.60 kg	179.47 kg	176.94 kg	0.89
220-bar transmission tower	6991.00 kg	7193.25 kg	7091.14 kg	64.73

5. Concluding remarks

In this paper, a novel method including MCTS with update process, the best reward, accelerating technique, and terminal condition has been formulated for sizing optimization of truss structures with discrete variables. The proposed method allows the agent to determine cross-sectional areas in each round. The following are the key points of this research:

- (1) An improved MCTS formulation with multiple root nodes is proposed. Once a design variable vector is determined in this round, this solution is used as the solution for initial state in next round. This process is called an update process.
- (2) The best reward of all nodes along the path is used in the backpropagation step. It is based on the maximum value between the current state value and the result of simulation.
- (3) Two kinds of accelerating techniques are used in this method: (1) The width of search tree is decreased as the update process proceeds. (2) The maximum number of iterations is reduced when more and more policy improvements are performed.
- (4) In each round, the agent is trained to find the solution under various constraints until the terminal condition is satisfied. When the improvement factor is less than 0.01%, the counter increases by 1. If the counter is greater or equal to 3, the algorithm terminates. Then, optimal solution is the minimum value of all solutions found by search trees during the algorithm.

It is verified from the numerical examples that the RL-based agent outperforms all algorithms in terms of the weight of the truss by introducing update process and the best reward. When accelerating technique is developed, the RL-agent requires very low computational cost. Moreover, this method is applicable for practical engineering problems because of MCTS.

The proposed method is expected to solve more complex problems such as simultaneous sizing, shape, and topology optimization of truss structures, which are our future research interests.

References

Altay, O., O. Cetindemir, and I. Aydogdu. 2024. "Size Optimization of Planar Truss Systems Using the Modified Salp Swarm Algorithm." *Engineering Optimization* 56 (4):

469-485. doi:[10.1080/0305215X.2022.2160449](https://doi.org/10.1080/0305215X.2022.2160449).

Browne, C. B., E. Powley, D. Whitehouse, S. M. Lucas, P. I. Cowling, P. Rohlfshagen, S. Tavener, D. Perez, S. Samothrakis, and S. Colton. 2012. "A Survey of Monte Carlo Tree Search Methods." *IEEE Transactions on Computational Intelligence and AI in Games* 4 (1): 1-43. doi:[10.1109/TCIAIG.2012.2186810](https://doi.org/10.1109/TCIAIG.2012.2186810).

Camp, C. V., and B. J. Bichon. 2004. "Design of Space Trusses Using Ant Colony Optimization." *Journal of Structural Engineering* 130 (5): 741-751. doi:[10.1061/\(ASCE\)0733-9445\(2004\)130:5\(741\)](https://doi.org/10.1061/(ASCE)0733-9445(2004)130:5(741)).

Christensen, P. W., and A. Klarbring. 2009. *An Introduction to Structural Optimization*. Berlin, Germany: Springer.

Duan, M. Z. 1986. "An Improved Templeman's Algorithm for the Optimum Design of Trusses with Discrete Member Sizes." *Engineering Optimization* 9 (4): 303-312. doi:[10.1080/03052158608902522](https://doi.org/10.1080/03052158608902522).

Eskandar, H., A. Sadollah, and A. Bahreininejad. 2013. "Weight Optimization of Truss Structures Using Water Cycle Algorithm." *International Journal of Optimization in Civil Engineering* 3 (1): 115-129.

Haftka, R. T., and Z. Gürdal. 1992. *Elements of Structural Optimization*. Berlin, Germany: Springer.

Hayashi, K., and M. Ohsaki. 2020. "Reinforcement Learning and Graph Embedding for Binary Truss Topology Optimization under Stress and Displacement Constraints." *Frontiers in Built Environment* 6: 59. doi:[10.3389/fbuil.2020.00059](https://doi.org/10.3389/fbuil.2020.00059).

Hayashi, K., and M. Ohsaki. 2021. "Reinforcement Learning for Optimum Design of a Plane Frame under Static Loads." *Engineering with Computers* 37: 1999-2011. doi:[10.1007/s00366-019-00926-7](https://doi.org/10.1007/s00366-019-00926-7).

John, K. V., C. V. Ramakrishnan, and K. G. Sharma. 1987. "Minimum Weight Design of Trusses Using Improved Move Limit Method of Sequential Linear Programming." *Computers & Structures* 27 (5): 583-591. doi:[10.1016/0045-7949\(87\)90073-3](https://doi.org/10.1016/0045-7949(87)90073-3).

Kocsis, L., and C. Szepesvári. 2006. "Bandit based Monte-Carlo planning." In *Proceedings of the 17th European Conference on Machine Learning*, pp 282-293.

Kooshkbaghi, M., A. Kaveh, and P. Zarfam. 2020. "Different Discrete ACCS Algorithms for Optimal Design of Truss Structures: A Comparative Study." *Iranian Journal of Science and Technology, Transactions of Civil Engineering* 44: 49-68. doi:[10.1007/s40996-019-00291-x](https://doi.org/10.1007/s40996-019-00291-x).

Kupwiwat, C., K. Hayashi, and M. Ohsaki. 2022. "Deep Deterministic Policy Gradient and Graph Convolutional Network for Bracing Direction Optimization of Grid Shells." *Frontiers in Built Environment* 8: 899072. doi:[10.3389/fbuil.2022.899072](https://doi.org/10.3389/fbuil.2022.899072).

Kupwiwat, C., K. Hayashi, and M. Ohsaki. 2024. "Multi-objective Optimization of Truss Structure Using Multi-agent Reinforcement Learning and Graph Representation."

Engineering Applications of Artificial Intelligence 129: 107594. doi:[10.1016/j.engappai.2023.107594](https://doi.org/10.1016/j.engappai.2023.107594).

Lee, K. S., Z. W. Geem, S. H. Lee, and K. W. Bae. 2005. "The Harmony Search Heuristic Algorithm for Discrete Structural Optimization." *Engineering Optimization* 37 (7): 663-684. doi:[10.1080/03052150500211895](https://doi.org/10.1080/03052150500211895).

Li, H. S., and Y. Z. Ma. 2015. "Discrete Optimum Design for Truss Structures by Subset Simulation Algorithm." *Journal of Aerospace Engineering* 28 (4): 04014091. doi:[10.1061/\(ASCE\)AS.1943-5525.000041](https://doi.org/10.1061/(ASCE)AS.1943-5525.000041).

Li, L. J., Z. B. Huang, and F. Liu. 2009. "A Heuristic Particle Swarm Optimization Method for Truss Structures with Discrete Variables." *Computers & Structures* 87 (7-8): 435-443. doi:[10.1016/j.compstruc.2009.01.004](https://doi.org/10.1016/j.compstruc.2009.01.004).

Luo, R., Y. Wang, W. Xiao, and X. Zhao. 2022a. "AlphaTruss: Monte Carlo Tree Search for Optimal Truss Layout Design." *Buildings* 12 (5): 641. doi:[10.3390/buildings12050641](https://doi.org/10.3390/buildings12050641).

Luo, R., Y. Wang, Z. Liu, W. Xiao, and X. Zhao. 2022b. "A Reinforcement Learning Method for Layout Design of Planar and Spatial Trusses using Kernel Regression." *Applied Sciences* 12 (16): 8227. doi:[10.3390/app12168227](https://doi.org/10.3390/app12168227).

Ororbia, M. E., and G. P. Warn. 2022. "Design Synthesis through a Markov Decision Process and Reinforcement Learning Framework." *Journal of Computing and Information Science in Engineering* 22 (2): 021002. doi:[10.1115/1.4051598](https://doi.org/10.1115/1.4051598).

Ororbia, M. E., and G. P. Warn. 2023. "Design Synthesis of Structural Systems as a Markov Decision Process Solved with Deep Reinforcement Learning." *Journal of Mechanical Design* 145 (6): 061701. doi:[10.1115/1.4056693](https://doi.org/10.1115/1.4056693).

Rajeev, S., and C. S. Krishnamoorthy. 1992. "Discrete Optimization of Structures Using Genetic Algorithms." *Journal of Structural Engineering* 118 (5): 1233-1250. doi:[10.1061/\(ASCE\)0733-9445\(1992\)118:5\(1233\)](https://doi.org/10.1061/(ASCE)0733-9445(1992)118:5(1233)).

Sadollah, A., A. Bahreininejad, H. Eskandar, and M. Hamdi. 2012. "Mine Blast Algorithm for Optimization of Truss Structures with Discrete Variables." *Computers & Structures* 102-103: 49-63. doi:[10.1016/j.compstruc.2012.03.013](https://doi.org/10.1016/j.compstruc.2012.03.013).

Sonmez, M. 2011. "Discrete Optimum Design of Truss Structures Using Artificial Bee Colony Algorithm." *Structural and Multidisciplinary Optimization* 43: 85-97. doi:[10.1007/s00158-010-0551-5](https://doi.org/10.1007/s00158-010-0551-5).

Sutton, R. S., and A. G. Barto. 2018. *Reinforcement Learning, Second Edition: An Introduction*. Cambridge, MA: MIT Press.

Świechowski, M., K. Godlewski, B. Sawicki, and J. Mańdziuk. 2023. "Monte Carlo Tree Search: A Review of Recent Modifications and Applications." *Artificial Intelligence Review* 56: 2497-2562. doi:[10.1007/s10462-022-10228-y](https://doi.org/10.1007/s10462-022-10228-y).

Templeman, A. B., and D. F. Yates. 1983. "A Segmental Method for the Discrete

Optimum Design of Structures.” *Engineering Optimization* 6 (3): 145-155. doi:[10.1080/03052158308902464](https://doi.org/10.1080/03052158308902464).

Wu, S. J., and P. T. Chow. 1995. “Steady-state Genetic Algorithms for Discrete Optimization of Trusses.” *Computers & Structures* 56 (6): 979-991. doi:[10.1016/0045-7949\(94\)00551-D](https://doi.org/10.1016/0045-7949(94)00551-D).

Yonekura, K., and Y. Kanno. 2010. “Global Optimization of Robust Truss Topology via Mixed Integer Semidefinite Programming.” *Optimization and Engineering* 11: 355-379. doi:[10.1007/s11081-010-9107-1](https://doi.org/10.1007/s11081-010-9107-1).

Zhu, S., M. Ohsaki, K. Hayashi, and X. Guo. 2021. “Machine-specified Ground Structures for Topology Optimization of Binary Trusses Using Graph Embedding Policy Network.” *Advances in Engineering Software* 159: 103032. doi:[10.1016/j.advengsoft.2021.103032](https://doi.org/10.1016/j.advengsoft.2021.103032).

Zhu, S., M. Ohsaki, K. Hayashi, S. Zong, and X. Guo. 2022. “Deep Reinforcement Learning-Based Critical Element Identification and Demolition Planning of Frame Structures.” *Frontiers of Structural and Civil Engineering* 16 (11): 1397-1414. doi:[10.1007/s11709-022-0860-y](https://doi.org/10.1007/s11709-022-0860-y).